2011

Magnetism of cluster-deposited Y–Co nanoparticles

Balamuruga Balamurugan

Ralph Skomski

Xingzhong Li

V. R. Shah

George C. Hadjipanayis

See next page for additional authors

Authors

Balamuruga Balamurugan, Ralph Skomski, Xingzhong Li, V. R. Shah, George C. Hadjipanayis, Jeffrey E. Shield, and David J. Sellmyer

Magnetism of cluster-deposited Y–Co nanoparticles

B. Balamurugan,[1,2,a)] R. Skomski,[1,2] X. Z. Li,[1] V. R. Shah,[1] G. C. Hadjipanayis,[3] J. E. Shield,[1,4] and D. J. Sellmyer[1,2]

[1]*Nebraska Center for Materials and Nanoscience, University of Nebraska, Lincoln, NE 68588, USA*
[2]*Department of Physics and Astronomy, University of Nebraska, Lincoln, NE 68588, USA*
[3]*Department of Physics and Astronomy, University of Delaware, Newark, DE 19716, USA*
[4]*Department of Mechanical Engineering, University of Nebraska, Lincoln, NE 68588, USA*

(Received 22 September 2010; accepted 15 November 2010; published online 22 March 2011)

Nanoparticles of YCo_2, YCo_3, and YCo_5 are produced by cluster-deposition and investigated both structurally and magnetically. The nanoparticles have sizes of less than 10 nm and are superparamagnetic at 300 K, irrespective of stoichiometry. As-produced nanoparticles exhibit disordered structures with magnetic properties differing from those of the bulk particles. The temperature-dependent magnetization curves of the nanoparticles reveal blocking temperatures from 110 to 250 K, depending on stoichiometry. The magnetic anisotropy constant K_1 of disordered YCo_5 nanoparticles of 7.8 nm in size is 3.5×10^6 ergs/cm^3, higher than those of the disordered YCo_2 (8.9×10^5 ergs/cm^3) and YCo_3 (1.0×10^6 ergs/cm^3) nanoparticles. © *2011 American Institute of Physics*. [doi:10.1063/1.3549602]

Since the discovery of a high uniaxial anisotropy field in YCo_5,[1] rare-earth cobalt (R-Co) bulk alloys, especially $SmCo_5$, have become important permanent-magnet materials. Such materials have high Curie temperatures ($T_c \geq 900$ K); appreciable magnetization ($4\pi M_s \sim 10\,000$ G); and high room-temperature anisotropies (K_1), from 5.5×10^7 ergs/cm^3 (YCo_5) to 22×10^7 ergs/cm^3 ($SmCo_5$).[1–4] Other Y–Co alloys, especially YCo_2 and YCo_3, have recently attracted much attention due to their intriguing magnetic properties.[5–10] Bulk YCo_3, a ferromagnetic material with a Curie temperature slightly above room temperature (307 K), has shown dramatic changes in its magnetic properties upon hydrogen absorption.[5–7] Bulk YCo_2 is a well-known exchange-enhanced Pauli paramagnet, [11,12] whereas the amorphous and nanocrystalline forms of YCo_2 have shown ferromagnetic behavior.[8–10]

Nanoparticles of R-Co have enjoyed considerable interest in recent years, especially with regard to their nanoscale magnetic properties and the exploration of these properties for future applications such as permanent magnets, magnetic recording media, etc.[13–15] However, the challenges in controlling the size, size-distribution, structure, and phase purity of the particles have limited this research to a few experimental studies, mostly based on surfactant-assisted wet chemical techniques. Generally, these studies focus on Sm–Co nanoparticles.[13–15] Furthermore, the presence of surfactants and the oxidation of these nanoparticles results in poor coercivity and substantial reduction in magnetization.[14,15] Bulk YCo_5 has been ball-milled to obtain nanocrystalline powders with relatively large particle sizes of 30 to 40 nm.[16] In the present study, we have used a plasma-condensation-type cluster-deposition method to produce YCo_2, YCo_3, and YCo_5 nanoparticles of much smaller sizes ($\leq$10 nm).

The experimental set-up, described elsewhere,[17,18] consists of a cluster-formation chamber that has a direct current (DC) magnetron plasma-sputtering discharge with a water-cooled gas-aggregation tube and a deposition chamber. A composite Y–Co target was sputtered using Ar and He as sputtering gases to form Y–Co nanoparticles in the gas-aggregation chamber; the nanoparticles were extracted as a collimated cluster beam traveling toward the substrate in the deposition chamber. The stoichiometry of these nanoparticles was controlled by varying the DC magnetron sputtering power (30 to 60 W) and composition of the target. The Y–Co nanoparticles were deposited on carbon coated Cu grids for transmission electron microscopy (TEM; JEOL 2010 with an acceleration voltage of 200 kV) and on Si substrates for SQUID magnetometer, energy dispersive x-ray analysis (EDX), and x-ray diffraction (XRD; Rigaku D/Max-B diffractometer) measurements.

The as-produced Y–Co nanoparticles have a spherical shape and an average particle size of about 9.0 nm, as shown in the TEM micrograph of the YCo_3 nanoparticles in Fig. 1(a). The selected-area-electron-diffraction (SAED) patterns in the inset of Fig. 1(a) show only two diffuse rings, revealing the disordered or amorphous-like structure. The average particle sizes of YCo_2 and YCo_5, estimated from the TEM micrographs, are about 9.6 and 7.8 nm, respectively. XRD also confirms the disordered structure of the Y–Co nanoparticles, irrespective of stoichiometry, as exemplified by the XRD pattern for YCo_3 [Fig. 1(b)], which has only two broad diffraction peaks in addition to the diffraction peak corresponding to the Si substrate. The standard data for the rhombohedral $PuNi_3$-type structure corresponding to the bulk YCo_3 are shown as lines in Fig. 1(b).[19] Note that the most intense diffraction peaks corresponding to bulk YCo_3 lie in the range of $2\theta = 40°$ to 50°, where the broad diffraction peak of the YCo_3 nanoparticles appears, as in Fig. 1(b).

In the cluster-deposition process, the inert gas ions impinging on the Y–Co target sputter the Co and Y atoms with

a)Author to whom correspondence should be addressed. Electronic mail: bbalasubramanian2@unl.edu.

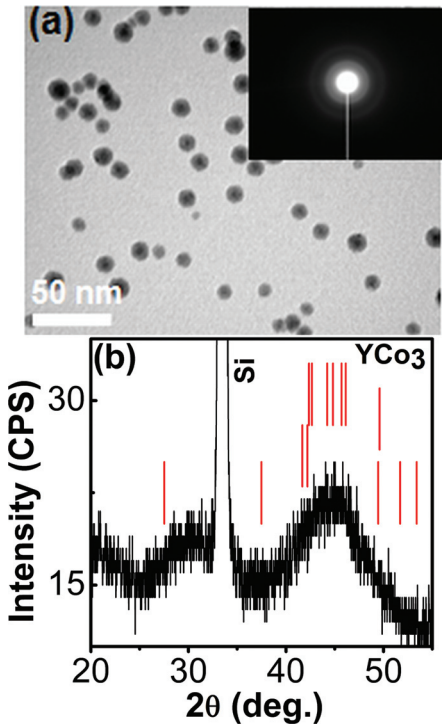

FIG. 1. (Color online) Structure of YCo_3 nanoparticles: (a) TEM micrograph, with selected-area-electron-diffraction pattern as an inset; and (b) x-ray diffraction pattern. The standard diffraction lines for bulk YCo_3 are presented as vertical lines.

a certain amount of energy. The sputtered atoms combine to form alloys by utilizing this energy, and they also lose the energy simultaneously by colliding with the inert gas atoms, until they reach thermal equilibrium. This process leads to the aggregation of Y–Co nanoparticles. The XRD and SAED patterns show that the energy acquired from the inert gas ions by Y and Co atoms is not sufficient to form a well-developed crystal lattice, leading to the disordered structure. Correspondingly, the XRD patterns of the YCo_2 and YCo_5 nanoparticles show a disordered structure, as compared to their bulk crystal structures.

The dependence of magnetization M of the YCo_2, YCo_3, and YCo_5 nanoparticles as a function of the applied magnetic field H was measured at 10 and 300 K. At 300 K, the nanoparticles show a very soft magnetic behavior, irrespective of their stoichiometry. For example, YCo_3 nanoparticles exhibit a very low coercivity H_c of 16 Oe and a remanence ratio M_r/M_s of 0.09 at 300 K [curve (i) in Fig. 2(a) and Fig. 2(b)]. These nanoparticles may therefore be superparamagnetic

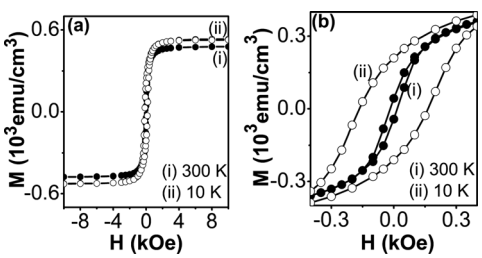

FIG. 2. Hysteresis of YCo_3 nanoparticles at (i) 300 K and (ii) 10 K: (a) full hysteresis loops and (b) expanded view.

and possibly lose their superparamagnetism due to the exchange interaction between them, leading to a very low room-temperature H_c and M_r/M_s. At 10 K, the coercivity and the remanence ratio values of the YCo_3 nanoparticles increase to 165 Oe and 0.39, respectively [curve (ii) in Fig. 2(a) and Fig. 2(b)]. Similar trends in the magnetization curves at 300 K and 10 K were also observed for the disordered YCo_2 and YCo_5 nanoparticles.

In order to study the properties of isolated Y–Co nanoparticles, the particles were exchange-decoupled by dispersing them in SiO_2. For this experiment, sequential depositions of Y–Co nanoparticle layer (~0.5 nm thickness) and SiO_2 layer (~8.5 nm thickness) were carried out, as is schematically shown in Fig. 3(a). The deposition of SiO_2 layers was performed using a radio-frequency magnetron-sputtering gun employed in the deposition chamber, and the total numbers of Y–Co and SiO_2 layers were 30 and 31, respectively. Fig. 3(b) shows that the YCo_2, YCo_3, and YCo_5 nanoparticles have zero coercivity at 300 K. At 10 K, the coercivity is nonzero (not shown).

Fig. 4 shows the zero-field-cooled (ZFC) and field-cooled (FC) magnetization curves of these exchange-decoupled Y–Co nanoparticles, measured in the temperature range of 5 to 300 K. The FC-ZFC curves confirm the superparamagnetic behavior of the Y–Co nanoparticles by showing the blocking temperature T_b, namely, about 110 K for YCo_2 and YCo_3 and 250 K for YCo_5.

YCo_2 is a well-known exchange-enhanced Pauli paramagnet, but nanocrystalline YCo_2 powders with particle sizes of 20 to 30 nm are soft-magnetic, with coercivities of 50 and 135 Oe at 300 and 35 K, respectively.[9] This has been attributed to the size-induced band narrowing at nanodimensions.[9] Bulk YCo_3 is a ferromagnetic material with a Curie temperature of 307 K.[5] In the present study, the YCo_2 and YCo_3 nanoparticles are smaller than 10 nm, so that thermal fluctuations induce superparamagnetic magnetization reversal.

By comparison, bulk YCo_5 ordered with the hexagonal $CaCu_5$-type structure is a ferromagnet with a high Curie temperature and a large magnetic anisotropy ($k_1 \sim 5.5 \times 10^7$ ergs/cm^3).[1,2] Crystallographically well-ordered YCo_5 nanoparticles should therefore be stable against thermal fluctuations and show a ferromagnetic signature at room temperature.[20]

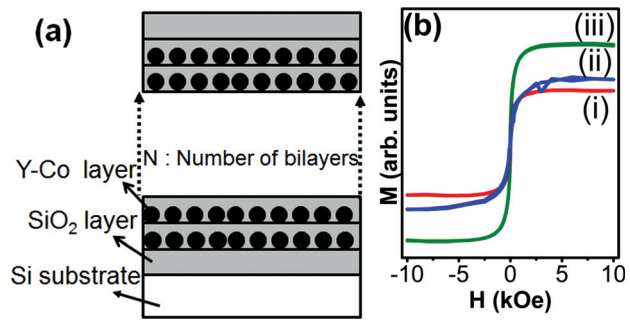

FIG. 3. (Color online) Exchange-decoupled Y–Co nanoparticles fabricated by a sequential deposition of nanoparticle (Y–Co) and matrix (SiO_2) layers: (a) schematic view and (b) room-temperature magnetization of the exchange-decoupled (i) YCo_2, (ii) YCo_3, and (iii) YCo_5 nanoparticles at 300 K. These curves reveal the superparamagnetic nature of the particles.

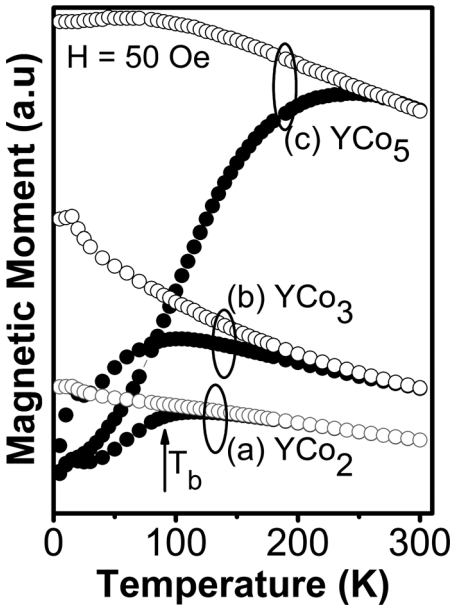

FIG. 4. Zero-field-cooled (solid spheres) and field-cooled (hollow spheres) magnetization curves for Y–Co nanoparticles dispersed in SiO_2 matrices.

However, in the present study, disordered YCo_5 nanoparticles with an average particle size of 7.8 nm show superparamagnetic behavior at room temperature (T_b of 250 K). This shows that the magnetic anisotropy of the disordered YCo_5 nanoparticles is lower than that of ordered YCo_5. We have evaluated the value of K_1 for the disordered YCo_5 nanoparticles using the relation $T_b = K_u V_p / 25 k_B$ for noninteractive single-domain particles, where K_u, V_p, and k_B are the anisotropy constant, the particle volume, and the Boltzmann constant, respectively. The result is 3.5×10^6 ergs/cm^3, much less than the bulk value but higher than the estimated K_1 values for disordered YCo_2 (8.9×10^5 ergs/cm^3) and YCo_3 (1.0×10^6 ergs/cm^3) nanoparticles.

In conclusion, we have used cluster-deposition to investigate YCo_2, YCo_3, and YCo_5 nanoparticles having sizes smaller than 10 nm. XRD and TEM results show that these nanoparticles have a disordered structure. The magnetic properties of the disordered Y–Co nanoparticles are very different from those of the corresponding bulk materials. The nanoparticles are superparamagnetic at 300 K and have nonzero coercivity at 10 K, irrespective of stoichiometry. The anisotropy of the disordered YCo_5 nanoparticles, as deduced from the blocking temperature, is much smaller than the bulk anisotropy.

ACKNOWLEDGEMENTS

This research is supported by ARPA-E (DE-AR 0000046, BB), BREM (BB, RS), DOE (DE-FG02-04ER46152, DJS, GCH), NSF-MRSEC (DMR-0820521, RS), ONR (JES, RS), and NCMN. Thanks are due to Z. Sun for technical assistance.

[1]K. Strnat, G. Hoffer, J. Olson, W. Ostertag, and J. J. Becker, J. Appl. Phys. **38**, 1001 (1967).
[2]R. Skomski and J. M. D. Coey, *Permanent Magnetism* (Institute of Physics, Bristol, 1999).
[3]L. N. Zhang, J. F. Hu, J. S. Chen, and J. Ding, J. Magn. Magn. Mater. **321**, 2643 (2009).
[4]I. A. Al-Omari, R. Skomski, R. A. Thomas, D. Leslie-Pelecky, and D. J. Sellmyer, IEEE Trans. Magn. **37**, 2534 (2001).
[5]A. Kashyap, R. Skomski, R. F. Sabiryanov, S. S. Jaswal, and D. J. Sellmyer, IEEE Trans. Magn. **39**, 2908 (2003).
[6]J. Liu, D. P. Broom, P. A. L. Georgiev, and D. K. Ross, J. Alloys Comp. 356–357, 174 (2003).
[7]X. Cui, J. Liu, P. A. Georgiev, I. Morrison, D. K. Ross, M. A. Roberts, K. A. Andersen, M. Telling, and D. Fort, Phys. Rev. B **76**, 184443 (2007).
[8]M. Ghidini, J. P. Nozieres, D. Givord, and B. Gervais, J. Magn. Magn. Mater. **140**, 483 (1995).
[9]S. N. Jammalamadaka, E. V. Sampathkumaran, V. S. N. Murthy, and G. Markandeyulu, Appl. Phys. Lett. **92**, 192506 (2008).
[10]S. D. Das, S. N. Jammalamadaka, K. K. Iyer, and E. V. Sampathkumaran, Phys. Rev. B. **80**, 192506 (2008).
[11]S. Khmelevskyi, P. Mohn, J. Redinger, and M. Weinert, Phys. Rev. Lett. **94**, 146403 (2005).
[12]Yu. S. Dedkov, C. Laubschat, S. Khmelevskyi, J. Redinger, P. Mohn, and M. Weinert, Phys. Rev. Lett. **99**, 047204 (2007).
[13]S. Stoyanov, V. Skumryev, Y. Zhang, Y. Huang, and G. Hadjipanayis, J. Appl. Phys. **93**, 7592 (2003).
[14]H. Gu, B. Xu, J. Rao, R. K. Zheng, X. X. Zhang, K. K. Fung, and C. Y. C. Wong, J. Appl. Phys. **93**, 7589 (2003).
[15]T. Matsushita, T. Iwamoto, M. Inokuchi, and N. Toshima, Nanotechnology **21**, 095603 (2010).
[16]N. Tang, Z. Chen, Y. Zhang, G. C. Hadjipanayis, and F. Yang, J. Magn. Magn. Mater. **219**, 173 (2000).
[17]B. Balasubramanian, K. L. Kraemer, N. A. Redding, R. Skomski, S. Ducharme, and D. J. Sellmyer, ACS Nano, **4**, 1893 (2010).
[18]Y. F. Xu, M. L. Yan, and D. J. Sellmyer, in *Advanced Magnetic Nanostructures*, edited by D. J. Sellmyer and R. Skomski (Springer, Berlin, 2006), p. 209.
[19]International Centre for Diffraction Data, Card No. 01-074-8441.
[20]B. Balamurugan, R. Skomski, X. Z. Li, and D. J. Sellmyer, Cluster Synthesis and Direct Ordering of Rare-Earth Transition-Metal Nanomagnets.